



Thermal and spectroscopic characterization of glass system $\text{PbO-CaO-B}_2\text{O}_3\text{-P}_2\text{O}_5$

N. Ait Hana, M. Taibi, J. Aride

*Université Mohammed V-Agdal, Laboratoire de Physico-Chimie des Matériaux Inorganiques et Organiques (LPCMIO),
Ecole Normale Supérieure Rabat Morocco*

Received 3 Aug 2014, Revised 11 Sept 2014, Accepted 11 Sept 2014
Corresponding author e-mail: taibiens@yahoo.fr

Abstract

The lead borophosphate glasses of general formula $\text{Pb}_{1-x}\text{Ca}_x\text{BPO}_5$ ($0 \leq x \leq 0.5$) were synthesized by conventional melting method. They were investigated by differential scanning calorimetry (DSC) and IR spectroscopy. The crystallization mechanism and kinetic parameters of crystal growth were evaluated using different models. It was found that the CaO takes a prominent part on the stability and on the nucleation phase of the glasses. According to obtained thermal parameters, the crystallization mechanism of the glasses depends on the calcium content. The analyses of IR spectra show that the CaO causes a change and stabilizes some phosphate and borate units in the structure of the borophosphate.

Keywords: Borophosphates, Glasses, Kinetic, Crystallization, IR spectroscopy

Introduction

In the last few years, a great deal of effort has been devoted to investigate the borophosphate and borosilicate glass materials in order to understand some specific properties of these materials. Lead borophosphate glasses have their part of interest; they possess an enhanced optical non-linearity due to high polarizability of Pb^{2+} ions in glass matrices [1, 2]. They are attractive materials for application in waveguides, optical switches and stimulated Raman amplifiers etc [3, 4]. Zinc-calcium borophosphate glasses were studied as candidates for applications as low-melting glass solders or glass seals [5, 6]. In a last work we have studied the glass forming region and the kinetic of crystallization in ternary system $\text{PbO-B}_2\text{O}_3\text{-P}_2\text{O}_5$ [7]. It has been established that the surface crystallization is dominant in this type of glasses.

In the present study, we report the role of CaO, substituting PbO, on the thermal parameters of lead borophosphate glasses. Thermal investigation and crystallization kinetics were carried out using differential scanning calorimetry. It was found that CaO takes a prominent part on the stability and in crystallization pattern of glasses. IR spectroscopy allows to determining the change of the network former of glasses as the CaO content.

2. Materials and methods

For this study we have chosen the following composition: $(1-x)\text{PbO-xCaO-0.5B}_2\text{O}_3\text{-0.5P}_2\text{O}_5$ with x ranging from 0 to 0.5 (in mol %). Analytical grade reagents of H_3BO_3 , PbO, $(\text{NH}_4)_2\text{HPO}_4$ and CaCO_3 powders in appropriate amounts were thoroughly mixed in an agate mortar, heated at about 200 °C for 24 h in a platinum crucible. The mixtures were annealed progressively to 600°C. The resulting compound is ground again and melted (between 800 and 1150°C, depending of CaO content) and then cooled on a metal plate preheated at 200°C. The obtained glasses are homogenous and transparent.

The samples were characterized by XRD technique (Siemens D5000 X-ray diffractometer employing Cu K α radiation) (figure 1). We can note that no line of diffraction is recorded for all synthesized materials, which confirms their amorphous state. Thermal study and kinetic of crystallization were carried out using a differential scanning calorimetry (DSC) type SETARAM 121 under argon flow. The measurements were conducted at various heating rates (5, 10, 15 and 20 °C/min) using approximately 20 mg of glass bulk in a Pt crucible.

The infrared spectra of glasses were recorded at room temperature using KBr disc technique. A Tensor 27 FTIR Bruker spectrometer was used to obtain the spectra in the wave number range 400 and 4000 cm^{-1} .

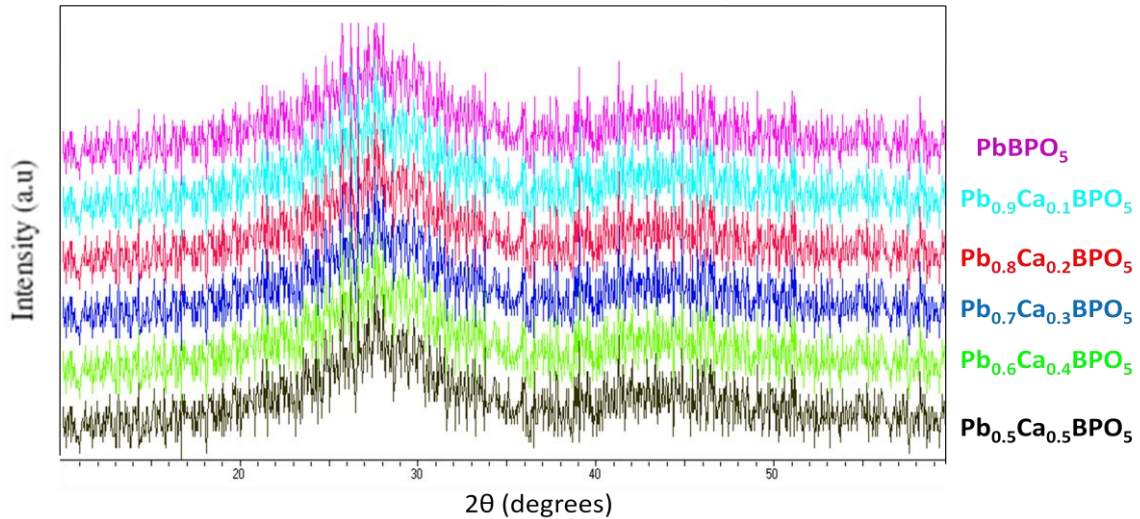


Figure 1: XRD patterns of $Pb_{1-x}Ca_xBPO_5$ ($0 \leq x \leq 0.5$) glasses.

3. Results and analysis

3.1. Thermal analysis

The DSC curves for the different stoichiometries of glassy system $Pb_{1-x}Ca_xBPO_5$ at heating rate $b = 10^\circ C \cdot min^{-1}$ were shown in figure 2. The behaviour of the thermograms depends of the composition of the glass. The thermograms indicate a change in the base line corresponding to the glass transition and an exothermic peak for crystallization process. T_g and T_c are respectively the glass transition and crystallization temperatures.

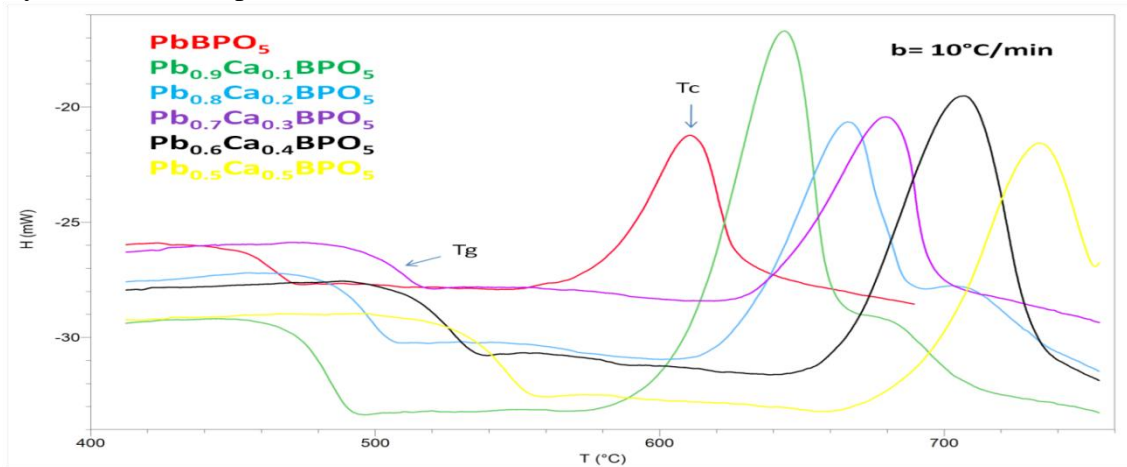


Figure 2: DSC curves for $Pb_{1-x}Ca_xBPO_5$ ($0 \leq x \leq 0.5$) Glasses at heating rate $b = 10^\circ C \cdot min^{-1}$

The values of T_g increase from $461^\circ C$ at the glass without CaO up $543^\circ C$ at the glass for $x = 0.5$. In table 1 were summarized the different thermal parameters for studied glasses. T_x is the onset temperature of crystallization peak. These parameters were determined to compute the thermal stability of the glasses from ΔT parameter, which is defined as $\Delta T = T_x - T_g$ [8].

Table 1: Thermal parameters of $Pb_{1-x}Ca_xBPO_5$ glass system

composition	T_g ($^\circ C$)	T_c ($^\circ C$)	T_x ($^\circ C$)	ΔT ($^\circ C$)
$x=0$	461	610	568	107
$x=0,1$	480	642	580	100
$x=0,2$	494	665	611	117
$x=0,3$	504	679	631	127
$x=0,4$	522	705	650	128
$x=0,5$	543	732	669	126

The variation of T_g and T_c versus CaO content at different heating rates is reported in figure 3. The increasing of both T_g , T_c and ΔT with CaO content confirm that the glasses were more stabilized when substituting PbO by CaO.

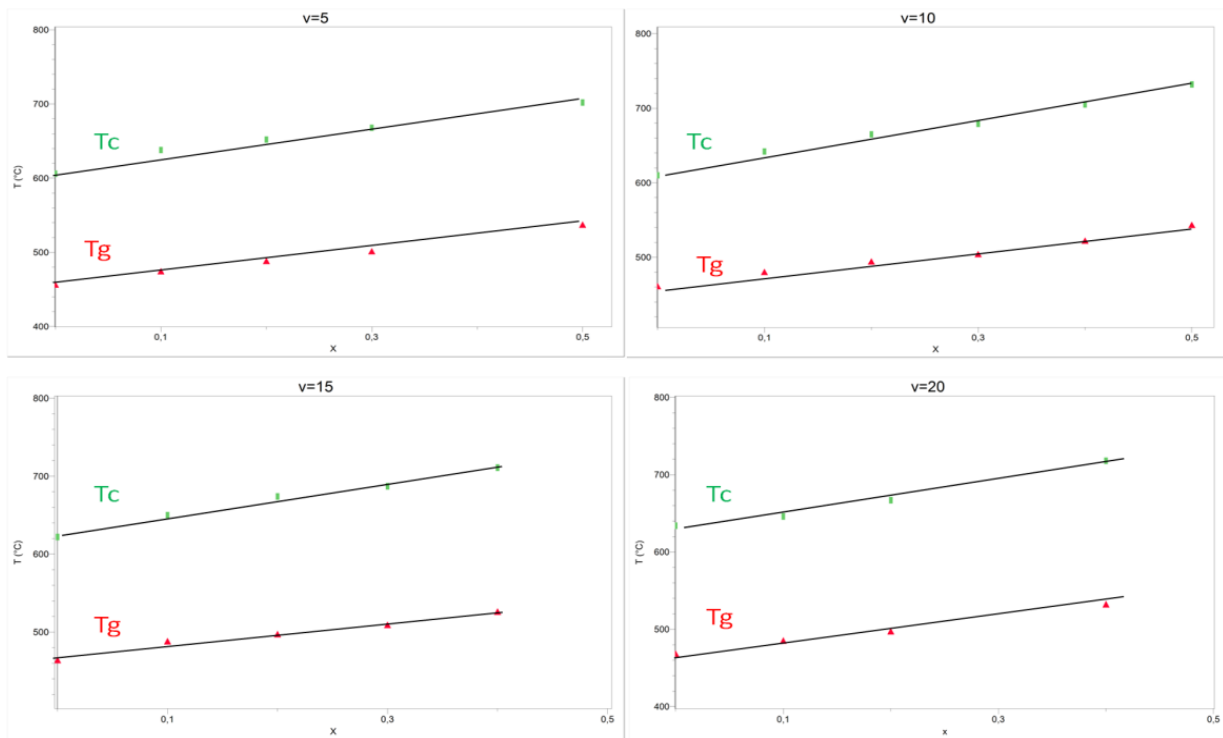


Figure 3: Variation of T_g and T_c as a function of CaO content in the glasses of $b= 5^\circ, 10^\circ, 15^\circ$ and $20^\circ\text{C}/\text{min}$.

3.2. Kinetic of crystallization

The calculation of crystallization kinetics were carried out for $\text{Pb}_{1-x}\text{Ca}_x\text{BPO}_5$ glasses with $x= 0, 0.3$ and 0.4 for different heating rates b (5 to $20^\circ\text{C min}^{-1}$). We have chosen these compositions for their single and complete crystallization peak. We note for the compositions $x=0.1$ and 0.2 , a second small exothermic peak due probably to the presence of an eutectic domain or to the non stoichiometry of the glass composition.

The kinetic parameters of studied glasses were determined using differential scanning calorimetry. We have used approach to non isothermal crystallization proposed by Kissinger [11,12]. The attractiveness of this model lies in the fact that, from the experimental point of view it requires readily accessible information on crystallization peak positions $T_p=T_c$, determined from a series of DSC scans taken at several heating rates b . The central equation of the Kissinger model is as follows [12]:

$$\ln\left(\frac{T_p^2}{b}\right) = \frac{E_a}{RT_p} + cte \quad (\text{Eq. 1})$$

Where b is the heating rate, T_p (Fig. 4) is the temperature corresponding to the maximum of crystallization peak, E_a is the activation energy of crystallisation process, R is the gas constant.

According to the Kissinger equation, a plot of $\ln(T_p^2/b)$ versus $1000/T_p$, (Fig 5), should be a straight line and the slope should be E_a/R . The crystallization mechanism may be correlated with the Avrami parameter by using the equation 2 [13].

$$n = (2.5 / \Delta T) RT_p^2 / E_a \quad (\text{Eq. 2})$$

Where ΔT is the width of the crystallization peak at half of its maximum.

On the other hand, we have used the modified Johnson-Mehl--Avrami equation to describe the behaviour of glass crystallization [14].

$$\ln[-\ln(1 - \alpha)] = -n \ln b - 1.052 \frac{mE_G}{RT} + \text{constante} \quad (\text{Eq.3})$$

In this equation, α is the crystallized fraction of the glass. It can be obtained directly from the DSC results by an analysis subroutine that integrates peaks to a specified temperature. α is estimated to S_T/S ; where S and S_T are respectively the total area of exothermic peak and the area of the peak at temperature T . n and m are numerical factors depending on the nucleation process and crystal growth morphology.

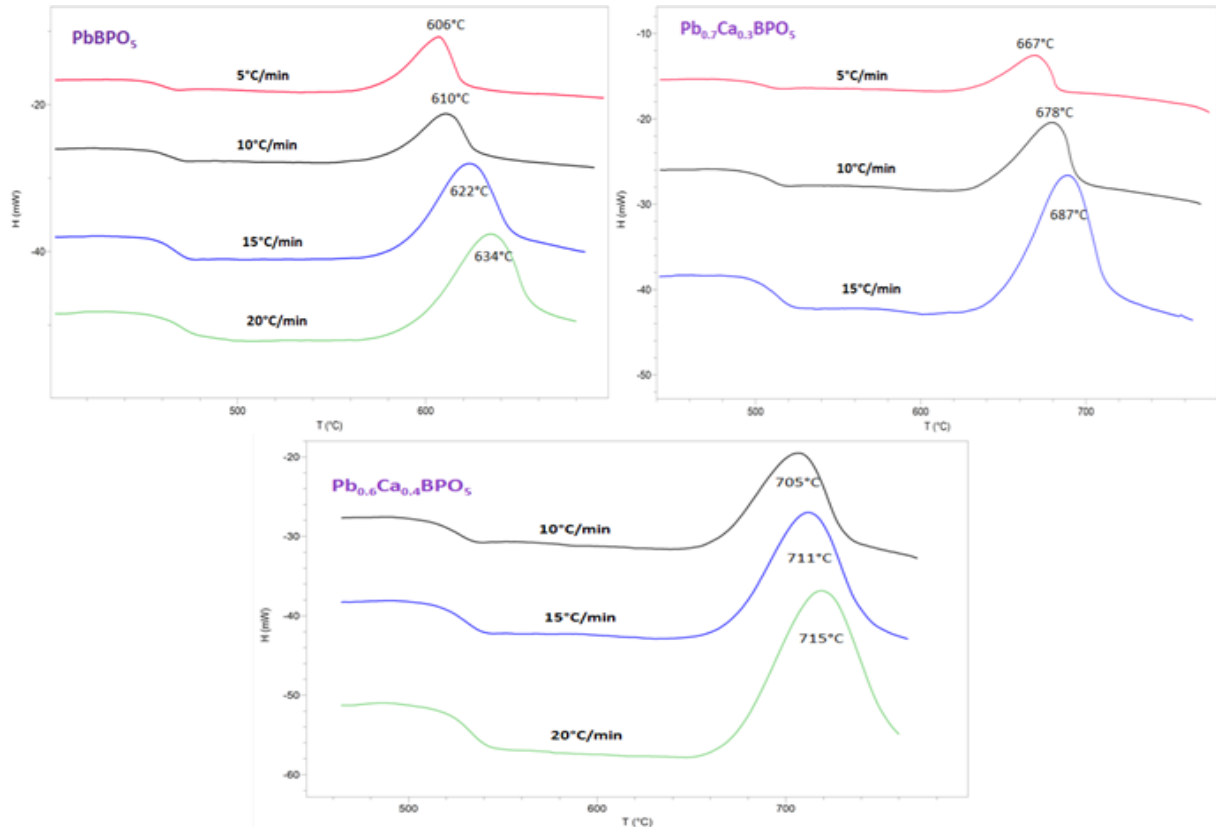


Figure 4: Temperature corresponding to the maximum of crystallization peak (T_p) for the $Pb_{1-x}Ca_xBPO_5$ ($x=0, 0.3$ and 0.4) glasses at different heating rates ($5, 10, 15$ and $20^\circ C \cdot min^{-1}$)

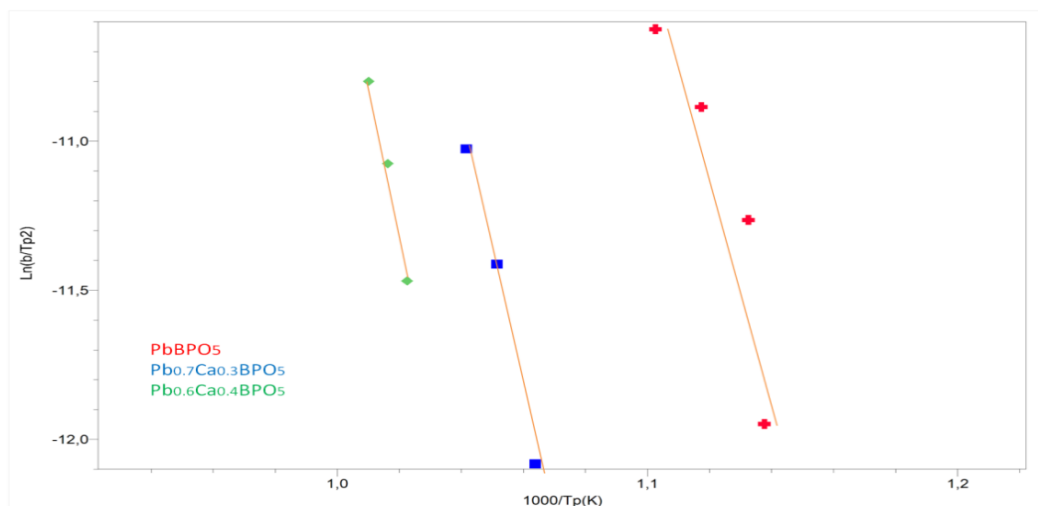


Figure 5: Kissinger plots ($\ln(b/T_p^2)$ vs. $1000/T_p$) for the $Pb_{1-x}Ca_xBPO_5$ ($x=0, 0.3$ and 0.4) glasses

The effective activation energy of the crystallization process is defined by $E_a = (m/n)E_G$. E_G and n can be given by Satava method for a constant heating rate b [15].

$$\left. \frac{d \ln [-\ln(1-\alpha)]}{d(1/T)} \right|_b = -1.052 \frac{mE_G}{R} \quad (\text{Eq.4})$$

And modified Ozawa-Chen method [16, 17]

$$\left. \frac{d(\ln b)}{d(1/T)} \right| = -1.052 \frac{m E_G}{n R} \quad (\text{Eq.5})$$

The plot of $\ln[-\ln(1-\alpha)]$ versus $1000/T$ (figure 6) allows to evaluate mE_G values.

The crystallized fraction α of studied glasses ($x=0.3$ and $x=0.4$) at different heating rates are shown on figure 7. The effective activation energy, $E_a = (m/n)E_G$, for the studied samples is deduced using Ozawa-Chen method by reproducing $\ln(b)$ as a function of $1000/T\alpha$ for different crystallized fraction α (Figure 8). The activation energy values are listed on table 2. The parameter n is calculated using the ratio mE_G/E_a .

The Kissinger curves $\ln(b/Tp^2)$ versus $1000/Tp$ (Eq.1) for $X= 0, 0.3$ and 0.4 are shown in figure 4. The corresponding activation energy from this method increases from 273.27 kJ/mol for $x= 0$ up 343.70 kJ/mol for $x= 0, 4$.

The different values of n , m and activation energy, indicate that CaO takes a prominent part on the crystallization mechanism of studied glasses.

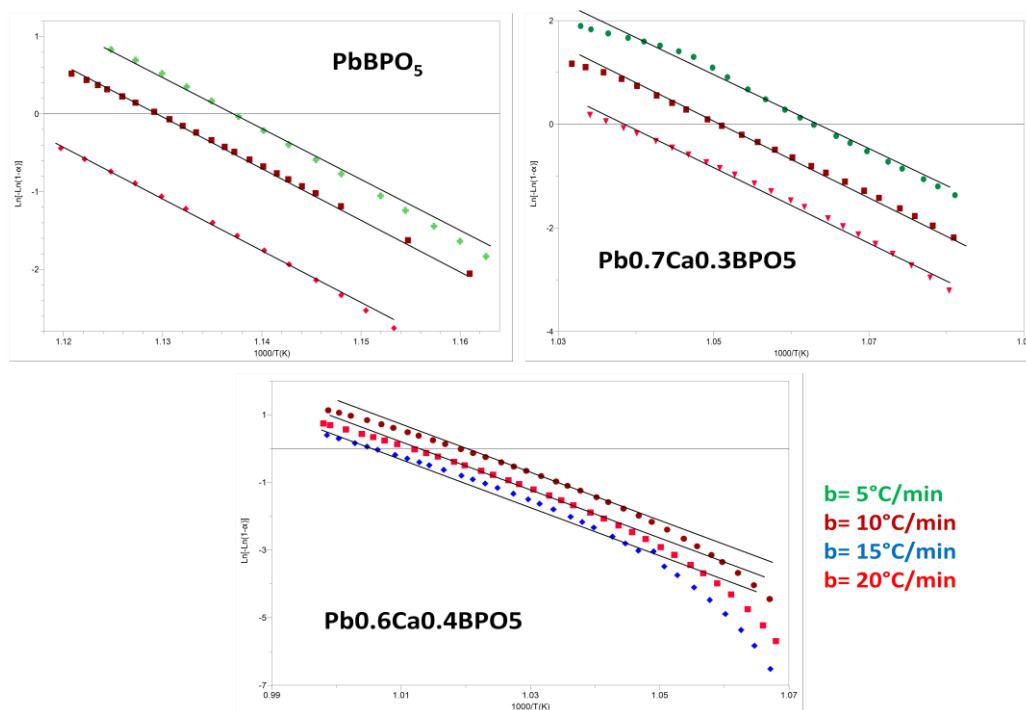


Figure 6: Satava method plots ($d\ln[-\ln(1-\alpha)]$ vs. $1000/T(K)$) for the $Pb_{1-x}Ca_xBPO_5$ ($x= 0, 0.3$ and 0.4) glasses

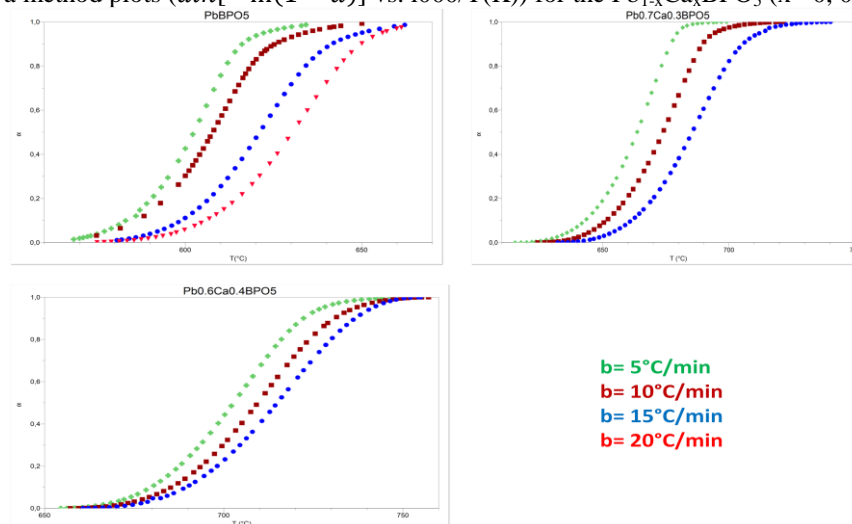


Figure 7: Fraction of crystallization α for the $Pb_{1-x}Ca_xBPO_5$ ($x= 0, 0.3$ and 0.4) glasses at different heating rates.

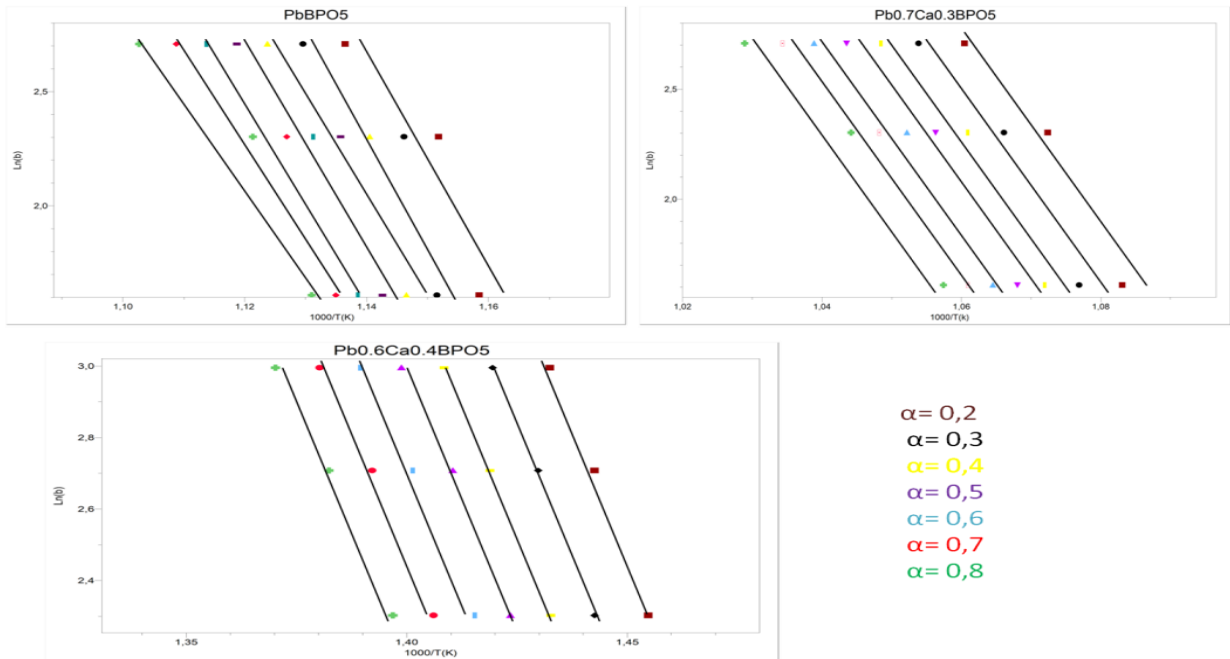


Figure 8: Ozawa-Chen plot ($\ln b$ vs. $1/T\alpha$) for $Pb_{1-x}Ca_xBPO_5$ ($x = 0, 0.3$ and 0.4)

Table 2: Kinetic parameters of crystallization of $Pb_{1-x}Ca_xBPO_5$ glass system calculated by different methods

Sample	Ozawa-Chen method				Kissinger method			
	n	m	E_G (kJ/mol)	E_a (kJ/mol)	E_a/R	E_a (kJ/mol)	ΔT	n
$PbBPO_5$	1.82	1	509.98	279.21	33.23	273.27	31.25	1.83
$Pb_{0.7}Ca_{0.3}BPO_5$	2.01	2	310	308.21	37.95	315.51	29	2.05
$Pb_{0.6}Ca_{0.4}BPO_5$	2.07	2	335.87	324.02	41.34	343.70	27.21	2.12

3.3 IR spectroscopy

The IR absorption spectra of $Pb_{1-x}Ca_xBPO_5$ glasses are reported on figures 9 and 10.

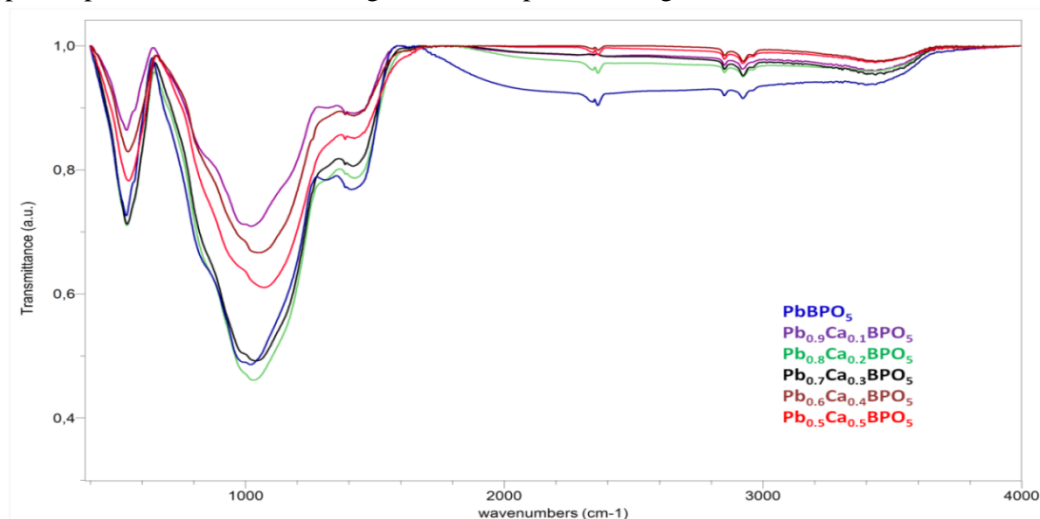


Figure 9: FTIR spectra of glasses $Pb_{1-x}Ca_xBPO_5$ ($0 \leq x \leq 0.5$)

It is evident that the behaviour of the spectra is characteristic of glassy form. The infrared spectra of glasses were recorded in the spectral range of $400-4000\text{ cm}^{-1}$. They are used to get more information about the presence of different structural groups. They are generally characterized by three distinguished regions. The first region extends from 1200 to 1500 cm^{-1} due to B–O stretching of BO_3 units, second region, from 800 to 1100 cm^{-1} , is

due to B–O stretching of both units BO4 and O–P–O angle (δ O–P–O). The third region lying around 500 to 600 cm^{-1} is due to the vibration of PbO. Besides that, the bands from 2400 to 4000 cm^{-1} are due to O–H vibration of the water group.

For the glass samples under study, the IR vibrations are mainly active in the mid-region of the infrared spectrum. The absorption bands are shown in the spectral range 1600 – 400 cm^{-1} (Fig. 10). The major observed absorption bands were summarized in table 3.

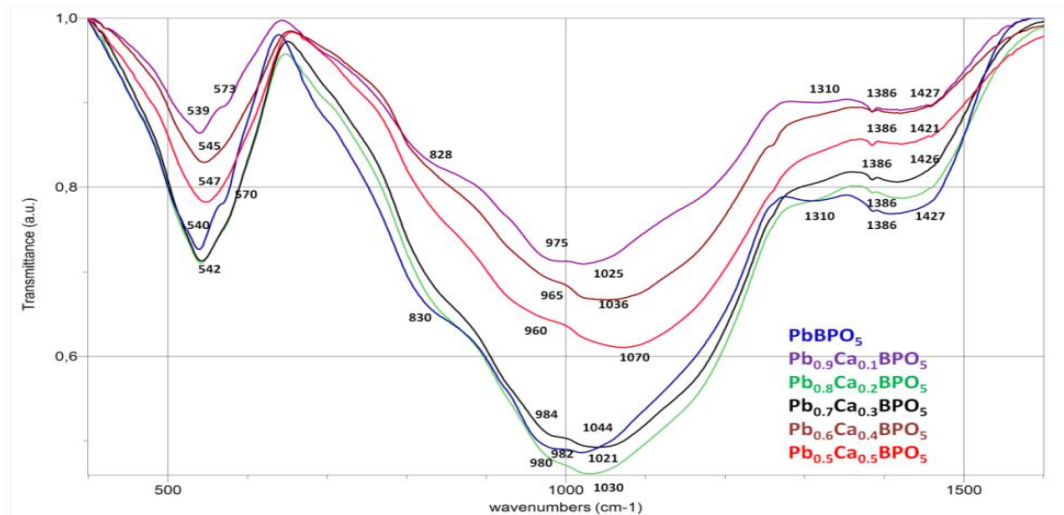


Figure 10: FTIR spectra of glasses $\text{Pb}_{1-x}\text{Ca}_x\text{BPO}_5$ ($0 \leq x \leq 0.5$)

Table 3: Data of infrared spectra of $\text{Pb}_{1-x}\text{Ca}_x\text{BPO}_5$ glasses

Glass Sample	Stretching vibration of B–O–B in [BO3] triangles			P–O–P asym. stretching	PO4 groups/ BO4 units	P–O–P sym. stretch	Vib of PbO	
PbBPO5	1428	1386	1310	1021	982	830	540	570
Pb _{0.9} Ca _{0.1} BPO ₅	1427	1386	1310	1025	975	828	539	573
Pb _{0.8} Ca _{0.2} BPO ₅	1425	1386	-----	1030	980	-----	542	----
Pb _{0.7} Ca _{0.3} BPO ₅	1422	1386	-----	1044	984	-----	542	----
Pb _{0.6} Ca _{0.4} BPO ₅	1421	1386	-----	1036	965	-----	545	----
Pb _{0.5} Ca _{0.5} BPO ₅	1422	1386	-----	1070	960	-----	547	----

4. Discussion

From the obtained data of thermal study, it is possible to make some conclusions for the competitive role of PbO and CaO in the stability of the studied glasses. One can see that an increase content of CaO leads to an increase of T_g , T_c and ΔT parameters (Table 1). Then CaO allows a thermal stability of the glasses and it is a potential network modifier. Following the results, the activation energy values increase from 273 kJ/mol for $x=0$ up 343 kJ/mol for $x=0.4$, confirming that CaO takes a strong role in the network of the glass structure at short distance. The different values of n and m (Table 2) indicate two different crystallization mechanisms. For $n=1$ means one-dimensional growth, $n=2$ means two-dimensional growth, $n=3$ means three-dimensional growth [22-23].

The average value of the crystallization order parameter, n , is equal to 1.83 for PbBPO₅ which suggests that there is one-dimensional stage in the start of the crystallization followed probably by a two-dimensional one. For Pb_{0.7}Ca_{0.3}BPO₅, Pb_{0.6}Ca_{0.4}BPO₅, n is equal to 2.05 and 2.12 respectively, suggests that there are two-dimensional (mostly confining to the surface of glass) crystallization processes taking place in these glass samples.

The infrared spectra analysis of borate network was carried out. Generally, the vibrational modes of the borate network are seen to be mainly active in three infrared regions, which were reported earlier. The first group of bands that occur at 1300–1500 cm^{-1} was due to the asymmetric stretching of borate units in which boron is connected to three oxygen. The second group observed at 900–1100 cm^{-1} , was due to B–O bonding stretching of B–O and P–O in the tetrahedral BO4 and PO4 units [18]. The third range recorded at 800–500 cm^{-1} is due to the symmetric stretching vibration of P–O–P bond and Pb–O–B bending vibration [19, 24, 25]. Infrared absorption

spectra of $Pb_{1-x}Ca_xBPO_5$ glasses (Fig.9 and 10), exhibit some changes with CaO content. We can note that the band observed in the region of $820-830\text{ cm}^{-1}$ assigned to P–O–P symmetric stretching vibrations became less pronounced or not recorded, in the spectra, for the glasses with high CaO content. This fact can be attributed to the breakup of the phosphate network with the formation of PO_4 units due to the introduction of calcium modifier. On the other hand the band found at 1310 cm^{-1} , assigned to stretching vibration of B–O–B in BO_3 groups, is not observed for the glasses with $x \geq 0.3$. As noted for the pyrophosphate units, CaO breaks the bridged bond in pentaborate chains to form ortho-borate units. It is evident that increasing the amount of CaO causes the spectral variations corresponding changes of the network structure. These changes are confirmed by the change in the crystallization kinetic of $Pb_{1-x}Ca_xBPO_5$ glasses. The modifier characteristic of CaO oxide, as confirmed from IR spectroscopy, leads to a change in the crystallization mechanisms of the studied glasses.

Conclusion

Various investigations such as differential scanning calorimetry (DSC), IR spectroscopy have been done to see the effect of calcium oxide in the structure of the borophosphate glasses. The study reveals that it is possible to prepare a wide composition range of glasses. Thermal study of borophosphate glasses showed that the calcium oxide has a strong role on the stability and in the crystallization mechanism. We have noted that the crystallization of glasses occurs in two phases. For glasses with high content of CaO ($x= 0.3, 0.4$), we have found two dimensional growth. The shape of the IR spectra is strongly influenced by the addition of CaO with a glass modifier characteristic. It is found that the addition of calcium to borophosphate glass structure involves a depolymerization of the phosphate and borate chains leading to the appearance of ortho-phosphate and orthoborate units.

References

1. Dimitrov V.V., Kim S.H., Yoko T., Sakka S., *J. Ceram. Soc. Jpn.*, 101 (1993) 59
2. Pan Z., Morgan S.H., Long B.H., *J. Non-Cryst.Solids*, 185 (1995) 127
3. Bogomolova L.D., Jachkim V.A., Dmitriev S.A., Stefanovsky S.V., *J. Non-Cryst. Solids*, 241 (1998) 174
4. Jana S., Karmakar B., Kundu P., *Mater. Sci. Poland*, 25(4) (2007) 1127
5. Koudelka L., Mosner P., Zeyer M., Jäger C., *J. Non-Cryst. Solids*, 326/327 (2003) 72
6. BrowR.K., *J. Non-Cryst. Solids*, 222 (2000) 396
7. Benali A., Taibi M., Aride J., Boukhari A., *Ann. Chim. Sci. Mat.*, S25 (2000) S131
8. Mahadevan S., Giridhar A., Singh A.K., *J. Non-Cryst.Solids*, 88 (1986) 11
9. Hruby A., *Phys. B*, 23 (1973) 1263
10. Hruby A., *Phys. B*, 22 (1972) 1187
11. Bansal N.P., Doremus R.H., *J. Therm. Anal.*, 29 (1) (1984) 115
12. Ray C.S, Day DE, *J. Am. Ceram. Soc.*, 67 (12) (1984) 806
13. Augis J.A., Bennett J.E., *J. Therm. Anal.*, 13 (1978) 283
14. Yinnon H., Uhlmann D.R., *J. Non-Cryst. Solids*, 54 (1983) 253
15. Satava V., *Thermochim. Acta*, 2 (1971) 423
16. Chen H.S., *J.Non-Cryst. Solids*, 27 (1978) 257
- 17- Ozawa T., *Bull. Chem. Soc. Jpn*, 38 (1965) 1881
18. Ravi Kumar A.V., Ch. Srinivasa Rao , G. Murali Krishna , V. Kumar , N. Veeraiah, *J. Molec. Struc.*, 1016 (2012) 42
19. Yoon Y., Park C., Kim J., Shin D., *Solid State Ionics*, 225 (2012) 637
20. Rada S., Culea M., Culea E., *J. Non-Cryst. Solids*, 354 (2008) 5493
21. Sherief M., *J. Non-Cryst. Solids*, 358 (2012) 411
22. Cheng Y., Xiao H., Guo W., *Ceramics International*, 33 (2007) 1345
23. Zhao H., Zhou W., Li Y., Wu J., *J. Am. Ceram. Soc.*, 85 (4) (2002) 903
24. EL-Egili K., Doweidar H., Moustapha Y.M., Abbas I., *Phys. B*, 339 (2003) 237
25. Mroczkowska M., Czeppe T., Nowinski J.L., *Solid State Ionics*, 179 (2008) 202

(2014) ; www.jmaterenvirosci.com